Computing single-particle flotation kinetics using automated mineralogy data and machine learning

Lucas Pereira, Max Frenzel, Duong Huu Hoang, Raimon Tolosana-Delgado, Martin Rudolph, Jens Gutzmer

Abstract

Flotation kinetic studies are essential for predicting, understanding, and optimizing the selective recovery of an ore through flotation. Recently, much effort has been put into incorporating intrinsic ore properties in the understanding of their flotation behavior. Particle-based characterization systems (e.g. automated mineralogy) drove much of this development. However, the currently available methods for flotation kinetic studies cannot accommodate single-particle data, and most of the available data end up not being used. Here we demonstrate a method to fit flotation kinetic models to each single particle characterized in a sample. Our method, based on the lasso-regularized multinomial logistic regression, allows for an in-depth understanding of a particle's flotation behavior according to every particle-descriptive variable available. We validate the efficiency of our new method in an apatite flotation case study that had been previously studied following traditional approaches. With the proposed method we can show the joint influence of particle size, shape, and modal and surface compositions in the recovery of single particles – such holistic understanding could not be captured before. We expect our method to help developing the field of flotation further and ultimately assist the implementation of more efficient mineral recovery plants – key for a more sustainable use of raw materials.

1 Introduction

Scanning electron microscope (SEM)-based automated mineralogy systems such as the mineral liberation analyzer (MLA) or TIMA-X have revolutionized the fields of process mineralogy and geometallurgy by providing particle-based characterization data at unprecedented resolution (Fandrich et al., 2007). Their development and application have had a considerable impact on the mining industry by improving the understanding of mineral separation processes, thus reducing investment risks (Gu et al., 2014). This is particularly true for complex ores (Frenzel et al., 2019; Kern et al., 2018; Lamberg and Vianna, 2007).

Despite its successful track record, the technique still holds considerable potential. This is so, because current best-practice process modelling tools are based on fitting particle distribution models (King et al., 2012), using only part of the available particle datasets. This is especially true for flotation, which is the most widely used mineral separation process in the mining industry. The complexity of the many microprocesses in flotation and their interactions hinders the development of process models that are capable of capturing most of the inherent complexity (King et al., 2012). The current use of particle data for modelling flotation kinetics is still insufficient to fully understand the process complexity since it loses much of the information contained in particle datasets with its required extensive data compression steps (e.g. particle binning and variable selection) (Gorain et al., 2000; Hoang et al., 2018; Jameson, 2012; Lamberg and Vianna, 2007; Lotter et al., 2011).

This contribution demonstrates a new method that extends the most recent developments in particle tracking (Pereira et al., 2020) to the modelling of flotation rate constants for individual particles. Such an approach has the potential to significantly improve the understanding and modelling of flotation processes by substantially increasing the resolution at which they are described.

1.1 Background

Most successful flotation models consider it as a kinetic process in analogy to chemical reactions (Dowling et al., 1985; King et al., 2012; Sutherland, 1948). In these models, the floatable mineral particles and the bubles are analogous to the reactant and the recovered mineral particles to the product. The transfer rate of particles from the pulp to the concentrate is a function of the probabilities of collision, attachment, and detachment of particles with, to and from bubbles (King et al., 2012). Various flotation kinetic models can be obtained by solving the equation of a kinetic rate process (Polat and Chander, 2000; Mesa and Brito-Parada, 2018):

Even though mathematical functions exist to quantitatively describe each of these probabilities at the micro-scale, their complexity and the number of free parameters they contain hold back their extensive application in flotation modelling (King et al., 2012; Polat and Chander, 2000).

Simplified models that describe particle recovery on the macro-scale while still considering flotation as a kinetic process are thus applied in practice (King et al., 2012; Polat and Chander, 2000). These models successfully capture the nature of the flotation process in a well-stirred flotation environment. A multitude of such simplified kinetic flotation models are available in the literature (Gharai and Venugopal, 2015; Polat and Chander, 2000). These models are obtained by solving the equation of a kinetic rate process (Eq. (1), Polat and Chander, 2000), where C and C_b are the concentrations of particles and bubbles, respectively, the exponents n and m are the reaction orders, t is time and k is the flotation rate constant.

$$\frac{dC}{dt} = -k_n C^n C_b^m \tag{1}$$

In regards to the material being processed, most of the differences between the available models reflect variations in the assumed distributions of mineral composition, mineral hydrophobicity and particle size (Polat and Chander, 2000). As demonstrated by Polat and Chander (2000), very good predictive accuracy can be achieved with simple flotation models when subdividing ore particles into classes of similar behavior. Thus, the classical first-order flotation rate constant model (Eq. (2), Sutherland, 1948) is one of the most widely used flotation models (q.v. Section 2.3). It models R_t, the recovery at time t, as a function of R_{max},the maximum recovery of a mineral phase at $t = \infty$, and its rate k:

$$R_t = R_{max}\left(1 - e^{-kt}\right) \tag{2}$$

To fit this kind of model to the behavior of a certain chemical element, mineral or particle class in a process, recovery needs to be determined as a function of time. This can be achieved with laboratory flotation experiments, or with a specific sampling campaign in industrial operations, designed to collect concentrate fractions corresponding to different flotation times (Runge, 2010; Wills and Finch, 2015). In the case of industrial operations, the continuous flotation kinetic models should be considered (Wills and Finch, 2015).

Subsequently, the recovery of component a in the concentrate at time t, R_t^a, can be calculated based on the grade of component a in the concentrate at time t, Ga_c^t, and in the original feed, Ga_f, as well as the masses of these two fractions, M_c^t and M_f:

$$R_t^a = \frac{M_c^t * Ga_c^t}{M_f * Ga_f} \tag{2}$$

Once recoveries as a function of time have been extracted for the relevant components, the optimal k and R_{max} parameters for each of these components can be obtained by fitting kinetic flotation models with a non-linear least squares analysis. Moreover, the goodness of the selected kinetic flotation fit for the compound can be evaluated with the obtained residuals (Wills and Finch, 2015).

To obtain the grades of chemical elements or minerals in the different materials, standard chemical (e.g X-Ray fluorescence, Jenkins, 2008) or mineralogical (e.g. X-ray powder diffraction, Bish and Post, 1989) bulk assays are sufficient. To obtain particle-level information, several techniques are available. For instance, laser-diffraction particle sizers can provide information on particle sizes. The most comprehensive particle-level data is generally provided by automated mineralogy systems. These are capable of characterizing the modal mineralogy, surface composition, size, and shape of individual particles in a sample (Fandrich et al., 2007), albeit with certain shortcomings due to stereologic degradation effects. These effects are co-responsible for the fact that the particles characterized in one sample cannot be directly matched to the particles characterized in other samples – i.e. particles observed on the feed cannot be identified with particles from the concentrate or the tailings. Thus, researchers have been binning particles with similar characteristics into a finite numbers of classes (e.g. via thresholds for free surface, particle size, or mineral association). These classes can then be used to calculate recoveries according to Eq. (2) and fit standard kinetic flotation models (Gorain et al., 2000; Hoang et al., 2018; Jameson, 2012; Lamberg and Vianna, 2007; Lotter et al., 2011).

Recently, Pereira et al. (2020) developed a new particle tracking method that extends this previous work and allows for computing the recovery probabilities of individual particles in mineral separation process with up to two output streams. The close link between such probabilities and bulk recoveries (Jowett, 1986; King et al., 2012; Tromp, 1937) provides the unique opportunity to understand particle flotation kinetics at the single-particle level. We present a method to perform particle tracking in mineral separation process with multiple output streams. The method allows us to compute a particle's cumulative recovery probability according to time, and ultimately fit flotation rate constant models to it. We obtain insights into the flotation process at an unprecedented level of detail.

We describe the method in detail in Section 2. Subsequently, its application is illustrated using real data from the flotation test work of Hoang et al. (2018) in Section 3. Finally, Section 4 presents a general discussion of the results together with an outlook of the method's impact.

2 Method

The method introduced in this manuscript fits flotation rate constant models to single particles by virtually simulating a flotation process, on a particle level. The method can be used at any scale, in laboratory, pilot or industrial scale.

First, even though no distinct flotation testing procedure is required, a brief overview on data acquisition is presented in Section 2.1. Following, the strategy to obtain the cumulative recovery of each particle in the feed sample over flotation time, essential information for fitting any kinetic flotation model to any type of component, is presented in Section 2.2. Lastly, Section 2.3 highlights important aspects of different flotation kinetic models available and advocates for the most suitable model to be used for particles. Figure 1 illustrates the method's workflow.

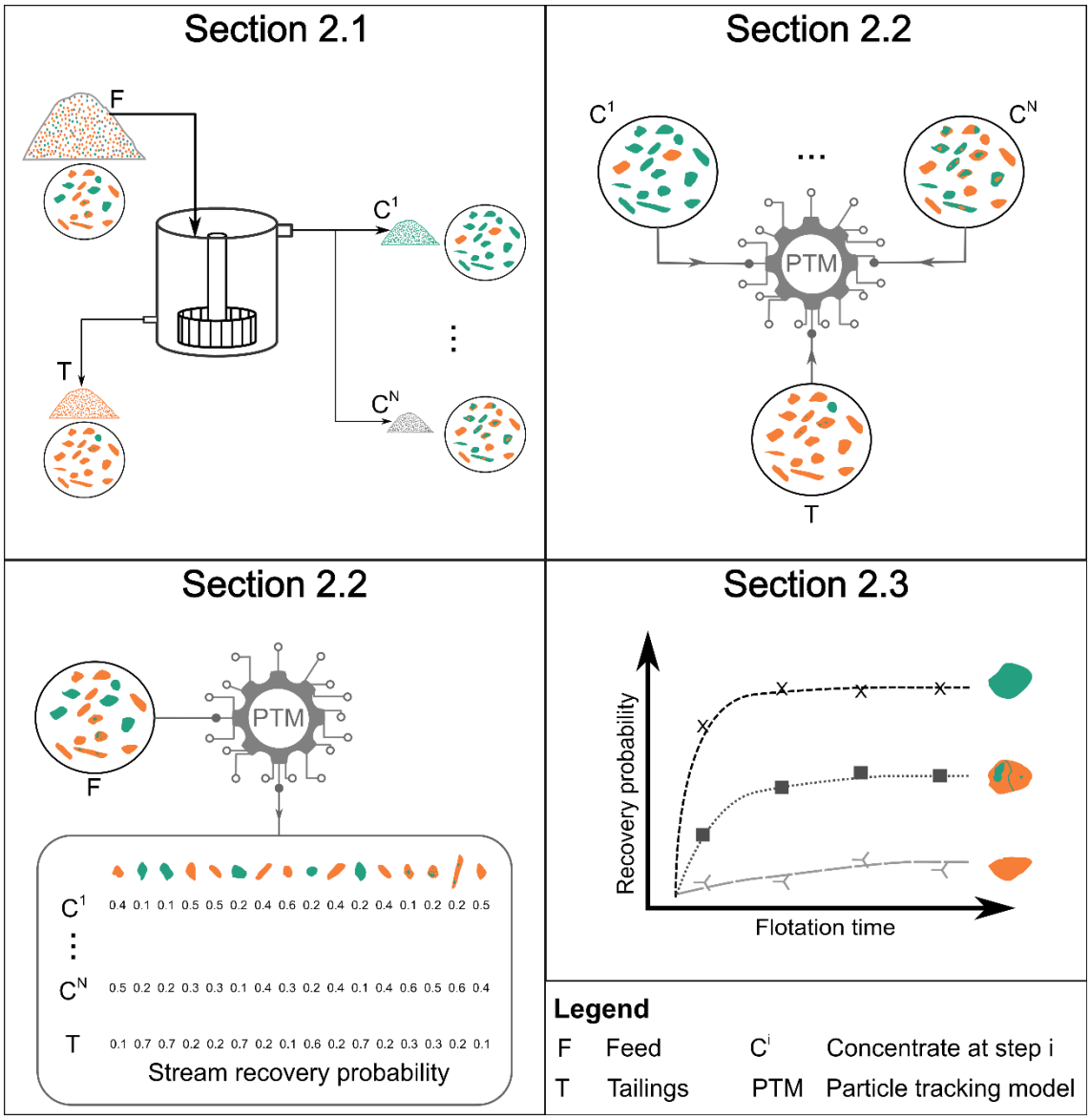

Figure 1: Workflow of the method. Boxes' headers indicate the section in which each step is explained.

2.1 Data collection

A similar sampling concept is required when developing flotation kinetics studies in a laboratory, pilot, or industrial scale: one must obtain different flotation concentrate samples along a studied flotation time range. In a standard laboratory batch test, sample collection is done by exchanging the froth collection tray at defined time intervals, while in the pilot or industrial scale, it is done by collecting a sample of the concentrate fraction at different flotation cells or banks (Runge, 2010; Wills and Finch, 2015).

Besides collecting one concentrate sample for each flotation time interval, our method also requires one sample from the tailings and one from the feed. We use the tailings sample for training the particle-based predictive model and the feed sample for validating it (q.v. Section 2.2). Moreover, kinetic flotation models are fitted to the particles in the feed sample, since they have not been used in the training phase. For more details on flotation test procedures, the reader is advised to refer to dedicated literature in the topic (Dobby and Savassi, 2005; Runge, 2010; Wills and Finch, 2015).

Following, particles in the collected samples need to be characterized according to their mineralogical composition, size, and shape. As discussed in Pereira et. al (2020), any characterization technique that delivers such information can be used. Automated mineralogy with the mineral liberation analyzer (MLA) is used in this study. No special characterization procedure is required and widely recognized literature on sample preparation and analysis is recommended (Fandrich et al., 2007; Heinig et al., 2015; Sandmann, 2015).

After characterization, the collected particle datasets are ready to be virtually processed. Due to the extent of data to be processed (ca. 150,000 particles per sample, each described by ca. 70 variables), the use of a programming environment is required. This manuscript follows the internal procedure of the Helmholtz Institute Freiberg for Resource Technology (HIF) to handle particle datasets in R (R Core Team, 2017), as introduced by Kupka et al. (2020). After importing the particle datasets, the particle descriptive variables in each dataset need to be treated according to their type (Pereira et al., 2020):

- Close (Pawlowsky-Glahn et al., 2015) the modal composition,
- Close the surface composition,
- Log-transform the enclosed circle diameter (ECD), solidity, and aspect ratio,
- Add the square of the log-transformed ECD as an extra variable (ECD^2).
- Add an interaction between every shape and size descriptive variables and a categorical variable indicating the main mineral in mass of each particle. This model structure, analysis of covariance (Keppel and Wickens, 2004), is used to capture a mineral-specific effect of particle dimension properties on its recoverability.

2.2 Particle cumulative recovery probability

Before proceeding with calculating the cumulative recovery probability of each particle, understanding the link between probability and recovery in flotation is required.

Summarizing the description of a flotation process given by King et al. (2012), each particle must collide with a rising bubble, adhere to the bubble, and not detach from it during the pulp, pulp-froth interface, and froth phases in order to be recovered. The most detailed flotation modelling equations quantify the recovery of particle bins (i.e. groups of particles with similar composition and physical properties) by calculating the rate at which each of these processes occurs. Yet, not every occurrence of these processes is successful, and given the complex nature of the microprocesses governing their chance of success, probabilities are used to quantify their efficiency (King et al., 2012). In summary, the properties of a particle influence their flotation behavior, the success of each interaction is random, and it can be described by probabilities.

In this work, probabilities are used as a measure of success of the macro flotation process, without breaking it up into collision, attachment, and detachment. The loss of

process resolution is compensated by the single-particle resolution as opposed to particle bins.

Real separation processes deal with a very large, that is, nearly an infinite number of particles. The individual particles characterized in the samples used for process analysis are actually a subset of this nearly infinite number of particles present in the real process. Identical particles have an identical probability of recovery, thus each particle characterized in the collected samples represents a bin of all other particles identical to it existing in the real system. The probability assigned to a particle in the analyzed sample represents the recovery of all particles of its type in the real system.

The method from Pereira et al. (2020) can be used to calculate the probability of each particle in a sample to be recovered in one of the product streams. As one of its strengths, the method can accommodate every particle property characterized with automated mineralogy, which later translates into an in-depth understanding of the influence of particle properties on its process behavior (q.v. Section 3.2.3). The exposition on that paper was, however, limited to two output streams. The method is thus extended in this contribution to accommodate several process streams, or concentrate fractions at different flotation time in the context of this manuscript.

The particle tracking method from Pereira et al. (2020) consists of training a least absolute shrinkage and selection operator (lasso)-regularized logistic regression model (Hastie et al., 2015) using a particle dataset from each process product obtained. In addition, it uses a prior probability adjustment step to accommodate for geological variability (Saerens et al., 2002). In our method, the lasso-regularized logistic regression is substituted by a lasso-regularized multinomial logistic regression (Hastie et al., 2015). This substitution allows for accommodating multiple classes (i.e. process products) while still being self-adaptive (i.e. no human input required) and able to accommodate for geological variability.

For obtaining the model's training data, one first has to bind into a single data frame the treated particle data from each concentrate and the tailings samples collected. Following, assign a statistical weight (Eq. 3) to each particle in the training dataset according to its original particle dataset. As represented in Eq. (3), the statistical weight ($SW_{p.sj}$) of each particle in sample *j* equals the bulk mass of this sample (W_{sj}) divided by the number of particles in its particle dataset (NP_{sj}) and the combined weight of the bound samples (W_t). The same concept can be used to reconstruct samples split into different size fractions; this topic is discussed in Annex 1.

$$SW_{p.sj} = \frac{W_{sj}}{W_t \cdot NP_{sj}} \tag{3}$$

According to the particle tracking method from Pereira et al. (2020), each class must be equally represented in the training dataset. In our case, we fulfill this requirement by normalizing the statistical weight assigned to the particles according to its given class to assure a 1:1 ratio between total statistical weights of every class.

The quality of each particle tracking model (PTM) should be evaluated before proceeding to the next steps. This procedure is explained in detail by Pereira et al. (2020). It consists of using bootstrapping (Henderson, 2005) to virtually simulate the mineral separation process multiple times. Resampling of the feed particle population (same number of particles, with replacement) is also done to evaluate sampling uncertainty. The grades and masses obtained for each process product, in each bootstrap run, are compared to the actual ones obtained in the test using a boxplot representation of natural log-ratios.

Ideally, they should not deviate significantly, indicating that sampling and modelling are reliable.

Following, we use the trained particle tracking model to compute the probability of each particle in the feed sample to be recovered in each concentrate fraction or to remain in the tailings. The cumulative sum of the probability of a particle to be recovered in the concentrate fractions is thus its cumulative recovery probability over flotation time. With this information, we can fit flotation kinetic models to each particle as detailed in Section 2.3.

2.3 Particle-based kinetic flotation model

A short review on the principles and assumptions of flotation kinetics, and thus the fundamentals of chemical reactions, is required for identifying the most suitable flotation kinetic model to be used for single particles. In the kinetics approach, flotation is considered a reaction between bubbles and particles (Polat and Chander, 2000). Despite much discussion about the order of this reaction, a first-order approach (Eq. (2)) has been used most extensively (Polat and Chander, 2000). The rate of a first-order chemical reaction depends linearly on the concentration of only one reactant (Petrucci et al., 2016), achievable in flotation if the availability of bubbles' surface area is constant (Polat and Chander, 2000).

In the set of first-order flotation kinetics models, each equation available has a unique flotation rate constant distribution function (Dowling et al., 1985; Polat and Chander, 2000). Many studies focused on identifying optimum distribution functions for the flotation rate constant of particle bins (Polat and Chander, 2000). Yet, Dowling et al. (1985) concluded that no single distribution function can be named "best", but the most suitable has to be identified for each case.

That can be explained by looking at the two factors controlling the distribution of the flotation rate constant: particle size and hydrophobicity. The singularities involved in the formation of different mineral deposits (Guilbert and Park, 2007) imply different mineralogical intrinsic properties (e.g. mineralogy, grain sizes, microstructure, and intergrowth relationships) to different ores, which are later translated into distinct distribution functions of particle size and hydrophobicity. Moreover, fitting distribution functions to the particles' intrinsic mineralogical properties is highly impaired by the non-trivial distribution of these properties: zero-inflated, skewed, and multimodal (Pereira et al., 2020). Therefore, Polat and Chander (2000) advocate for grouping particles into bins of similar behavior (i.e. similar intrinsic properties) and use a flotation model with simple flotation rate constant distribution function.

In our method, we capture the individual behavior of each characterized particle, which might be understood as using the maximum number of particle bins possible (q.v. Section 2.2), thus justifying the use of the classical first-order model (Eq. (2), Sutherland, 1948) – the flotation kinetic model of simplest flotation rate constant distribution.

3 Demonstration

We demonstrate here the ability of our method on the flotation case study of Hoang et al. (2018). First, the case study is presented in Section 3.1. Following, we validate the quality of the trained particle tracking models in Section 3.2.1, and of the flotation kinetic model fitted to each particle in Section 3.2.2. Lastly, we use the results obtained to understand the influence of particle properties on their flotation behavior in Section 3.2.3.

In this context, the R_{max} and k obtained for each particle is used to calculate the modified flotation rate constant (k_m) introduced by Xu (1998). k_m corresponds to the product of k and R_{max}; it represents the slope of the tangent of the recovery-time curve at zero time, and is used since some operating conditions can affect R_{max} but not k, and vice-versa. Thus, k_m provides a better insight on the influence of each particle property (e.g. mineral composition, liberation, size, shape, etc.) on a particle's overall flotation behavior.

3.1 Materials and methods

Phosphate rock samples from the Lao Cai province in Vietnam were provided for the study of Hoang et al. (2018) by the Vietnam Apatite Limited Company. The objective of the experiment was to selectively separate fluorapatite from dolomite, calcite and silicates. Sampling and crushing procedures are available in Leißner et al. (Leißner et al., 2016).

Table 1 displays the modal composition of the feed sample. Twenty three minerals were identified with the MLA and grouped into apatite, dolomite, calcite, micas, other silicates, sulfides, and oxides in the following sections, figures and tables for better visualization. Phlogopite, quartz, pyrite, and hematite, respectively, are the main minerals of the multi-mineralic groups. The apatite grade of the ore is high (64.1 wt.%) and dolomite is the main gangue mineral (20.7 wt.%).

Table 1: Grouped modal mineralogy of the feed sample, obtained with the MLA

	Apatite	Dolomite	Calcite	Other silicates	Micas	Sulfides	Oxides
Feed (wt.%)	64.1	20.7	6.1	5.6	2.4	1.1	0.1

After grinding for 8 minutes in a laboratory ball mill to assure a d90 of 67 µm, batch flotation tests were performed in a flotation cell built at the TU Bergakademie Freiberg. Corn starch ($(C_6H_{10}O_5)_n$) gelatinized with sodium hydroxide (NaOH) was used in combination with sodium silicate (Na_2SiO_3) to depress gangue minerals. The latter also acts as a fine particle dispersant. Solution pH was kept at 10 using sodium carbonate (Na_2CO_3). Berol 2015 was used as collector. Four concentrate fractions were collected over the 0.00-0.75 min (CA), 0.75-1.50 min (CB), 1.50-3.00 min (CC), and 3.00-6.00 min (CD) time intervals. In addition, a final tailings sample was collected (TD). Five replicates of the test were done to ensure reproducibility and produce enough sample mass for detailed characterization.

Each flotation product and the feed samples were wet sieved into four size fractions (-20, +20 to -32, +32 to -50, and +50 µm) before characterization by MLA at the Helmholtz Institute Freiberg for Resource Technology. Samples were prepared following the procedure described by Heinig et al. (2015), and analyzed on a FEI Quanta 650F scanning electron microscope equipped with two Bruker Quantax X-Flash 5030 EDX detectors with a 25 kV overall electron beam accelerating voltage and X-ray Back Scattered Electron measurement mode. MLA results were validated with ICP-OES chemical assays. More details on the flotation and analytical procedures are available in Hoang et al. (2018).

Table 2 presents the weight distribution of the five flotation products collected together with the number of particles in their respective MLA datasets, the class-label, and statistical weight used in the training phase of the particle tracking model. The R package glmnet is used to train the lasso-regularized multinomial logistic regression (Friedman et

al., 2010). Annex 1 presents in detail the statistical weight assignment procedure applied to these samples given that they were split into several size fractions.

Table 2: Weight distribution, number of particles characterized with the MLA, label, and statistical weight assigned to flotation each product for training the particle tracking model

Sample	Wt. (%)	Particle nº	Assigned label	Statistical weight
CA -20	6.7	185952	CA	2.29E-04
CA 20-32	5.8	212465	CA	1.73E-04
CA 32-50	4.6	137023	CA	2.15E-04
CA +50	2.2	78712	CA	1.79E-04
CB -20	6.4	173513	CB	2.39E-04
CB 20-32	5.4	198645	CB	1.77E-04
CB 32-50	3.9	142061	CB	1.78E-04
CB +50	2.8	86449	CB	2.11E-04
CC -20	5.8	164071	CC	2.57E-04
CC 20-32	4.3	184961	CC	1.68E-04
CC 32-50	3.5	139719	CC	1.82E-04
CC +50	2.0	76500	CC	1.88E-04
CD -20	4.7	148161	CD	2.86E-04
CD 20-32	2.8	164470	CD	1.54E-04
CD 32-50	2.3	117546	CD	1.73E-04
CD +50	1.1	61203	CD	1.68E-04
TD -20	11.3	124433	TD	2.84E-04
TD 20-32	7.0	199521	TD	1.06E-04
TD 32-50	6.7	156597	TD	1.34E-04
TD +50	10.7	73710	TD	4.55E-04

3.2 Results

3.2.1 Particle tracking models and validation

Figure 2 displays boxplots comparing the predicted to the actual mass and mineralogical composition values of each concentrate and the final tailings using natural log ratios. The accessory mineral groups (oxides, sulfides, and micas) display the highest variability in the modelling results. Even though the median mass predicted for the first and fourth concentrate show a substantial deviation from their actual values (ca. 30%), the tailings mass (and thus, its complementary, the total recovered mass) as well as most of the major components are correctly predicted, and the models are therefore considered satisfactory. Particularly, the results for apatite, the ore mineral, and carbonates are excellent.

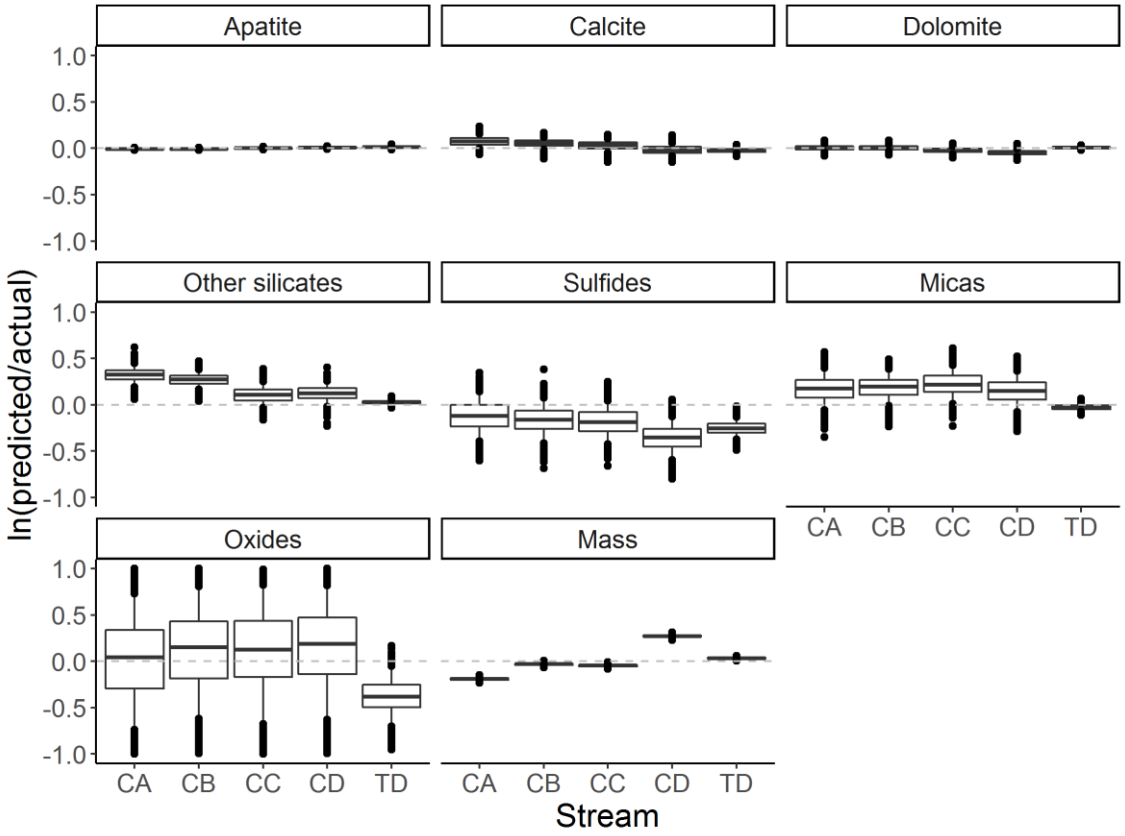

Figure 2: Boxplots comparing the predicted and actual flotation product's mass and composition using natural log ratios. Center lines represent the median, boxes represent the 0.25 and 0.75 percentiles, and whiskers the 0.05 and 0.95 percentiles. Dots represent the values beyond these thresholds, the outliers.

3.2.2 Flotation kinetics of single particles

A classical flotation kinetic model was fitted to each particle using the calculated cumulative recovery probability. Figure 3 is used to evaluate the quality of the fit for 49 randomly selected particles by comparing their computed recovery probability to the fitted kinetic model. Figure 4 displays the standard regression error of k and R_{max} for all particles. The median error of k is ca. 0.05 min^{-1} and of R_{max} is ca. 4.5 %. Clearly, the classical first-order flotation model successfully fits the recovery probability trend of each particle.

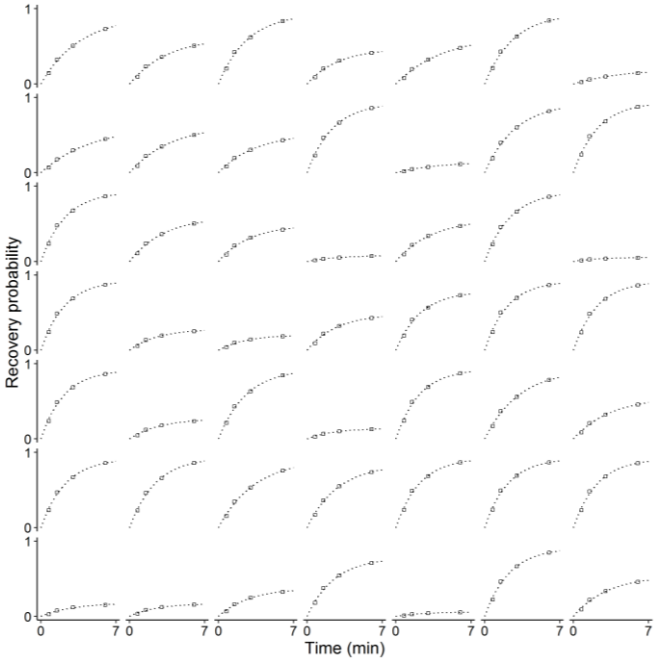

Figure 3: Comparison between calculated recovery probabilities (dots) and the classical kinetics flotation model (dotted line) fitted to 49 random particles.

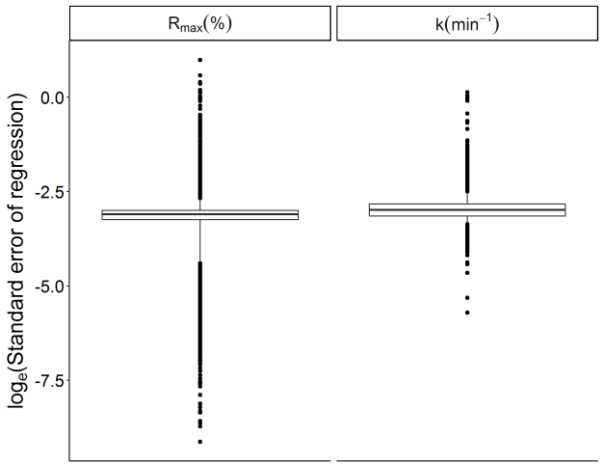

Figure 4: The natural logarithm of the standard regression error of k and Rmax for all particles represented as boxplots. Center lines represent the median, boxes represent the 0.25 and 0.75 percentiles, and whiskers the 0.05 and 0.95 percentiles. Dots represent the values beyond these thresholds, the outliers.

Figure 5 displays the distribution of k_m for the different particles according to their main mineral in mass. As expected, apatite-rich particles have a higher k_m (i.e. better process performance) than the gangue-rich ones: the median k_m of apatite-rich particles, ca. 0.38 min^{-1}, is more than two times higher than the median k_m of calcite- and dolomite-rich particles, ca. 0.16 min^{-1}, and seven times higher than that of phlogopite and quartz, ca. 0.06 min^{-1}. These results also indicate a more efficient separation of apatite from silicates in comparison to carbonates, from this apatite ore due to similarities in surface properties between the semi-soluble salt-type carbonates and calcium phosphate minerals.

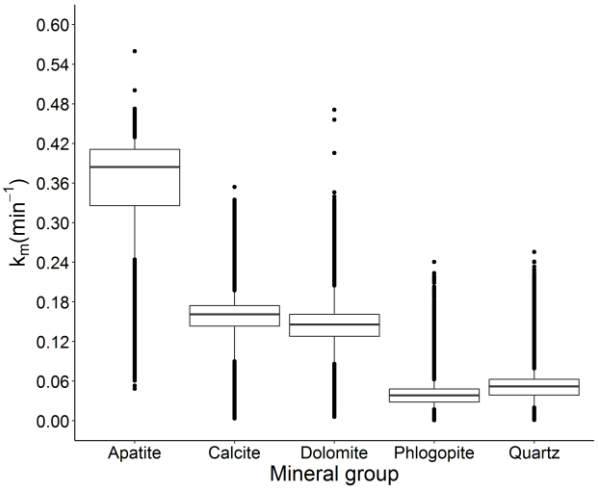

Figure 5: k_m distribution boxplots of particles according to their main mineral component. Center lines represent the median, boxes represent the 0.25 and 0.75 percentiles, and whiskers the 0.05 and 0.95 percentiles. Dots represent the values beyond these thresholds, the outliers.

3.2.3 Influence of particle properties

For simplifying the analysis of particle properties influencing the process behavior, only the predominant minerals of the major mineral groups are considered. When analyzing these results, one must bear in mind that k_m*'s* distribution is predominantly caused by particle properties, but part of the observed variability derives from the probabilistic approach used in this method.

Figure 6 displays the distribution of k_m values among fully liberated (surface based) particles of the main minerals according to particle size and aspect ratio. The expected quasi-parabolic, "the elephant curve in flotation", size influence on recovery is clearly depicted for apatite, dolomite and calcite. The carbonate minerals reach their maximum k_m at ca. 10 µm – a finer size range in comparison to apatite (ca. 30 µm). While apatite, the mineral with highest hydrophobicity in this experiment, is mainly recovered by true flotation, dolomite and calcite, the less floatable minerals, can end up in the concentrate partly by true flotation or by entrainment. Quartz and phlogopite particles are being recovered by entraintment in this test. In this test, we did not observe the influence of solidity in the k_m of single particles.

Figure 7 displays the influence of particle size, liberation, aspect ratio, and association on the k_m of particles containing apatite. Visibly, the poorly liberated apatite particles display a k_m trend very similar to that of their main associated mineral, as depicted in Figure 6. Also, particles with liberation degree higher than 70% exhibit a similar k_m trend to fully liberated apatite particles (Figure 6). Finally, particles in the intermediate liberation bin show a clear bimodal k_m distribution. The aspect ratio influence is less evident for non-liberated particles (Figure 7) than for the fully-liberated ones (Figure 6).

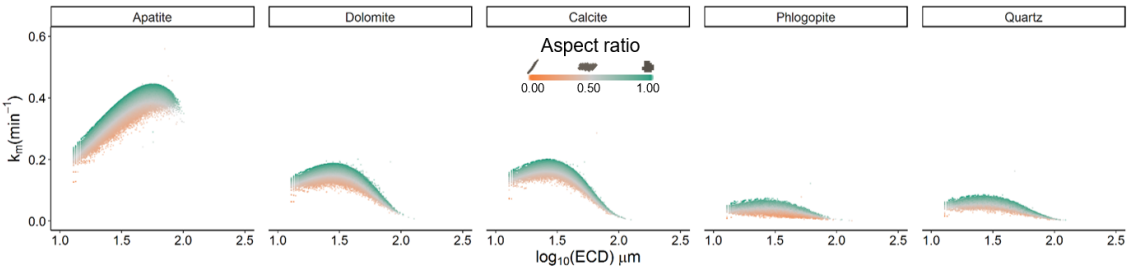

Figure 6: Distribution of k_m among fully liberated particles (surface composition), according to their particle size (enclosed circle diameter - ECD.

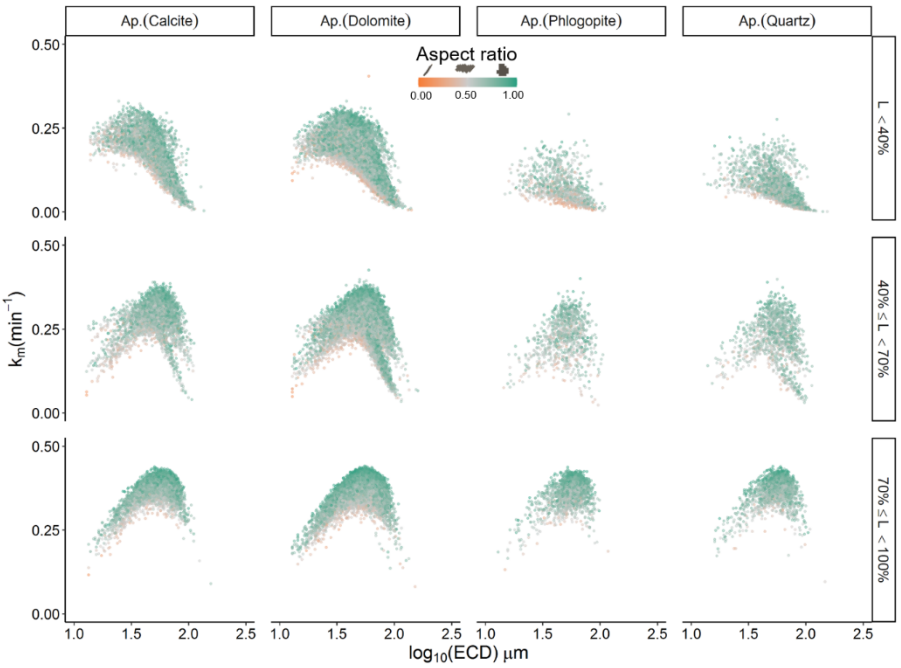

Figure 7: Distribution of k_m among particles containing apatite, according to their size (enclosed circle diameter - ECD), liberation degree (L), and aspect ratio. Particles are further grouped according to their main association, as indicated in parentheses.

4 Discussion and final thoughts

This contribution successfully extends the particle tracking method from Pereira et al. (2020) to a multinomial framework where the probability of a particle to be recovered in more than two output streams can be computed. The new method allows for calculating the cumulative recovery probability of each particle in a flotation setup. This information allows for fitting flotation kinetic models to single particles, a breakthrough in the study of flotation. We demonstrate the method on a batch flotation test, nevertheless it is applicable to pilot or industrial flotation operations with proper sampling procedures. In addition, it enables the use of particle tracking on mineral separation setups with more than two output streams (e.g. shaking table).

The method captured recovery trends similar to those observed by (Hoang et al., 2018). Apatite particles show the best flotation behavior as described by their k_m. The system is more selective towards silicates than carbonates. The maximum k_m of apatite is obtained at ca. 30 µm particle size. The k_m of phlogopite and quartz decrease with size, indicating that entrainment is possibly their major recovery mechanism. Yet, the particle tracking approach delivers a much more detailed insight of the flotation process.

Figure 8 presents the recovery of particles containing apatite following the traditional particle binning approach (A, Hoang et al., 2018) and the new particle-based method (B). Since the characterized particles were not binned in the particle-based approach (Figure 8 B), it displays a much more detailed recovery probability distribution than the traditional one (Figure 8 A). In addition, the new method avoids bin representativity issues commonly present in the particle binning approach.

As discussed by Hoang et al. (2018), some incongruent results arise from the low representativity of particles in some size/liberation bins. For example, fully liberated apatite particles show the highest recovery in comparison to other liberation bins in every size bin but the finer one (size < 20µm, Figure 8 A). The authors attributed this divergence to the agglomeration of fine particles during sample preparation, which unbalanced the fine particle distribution among the different liberation bins. The multinomial logistic regression avoids this issue by capturing the influence of each particle property on its process behavior, continuously, over the entire property distribution space.

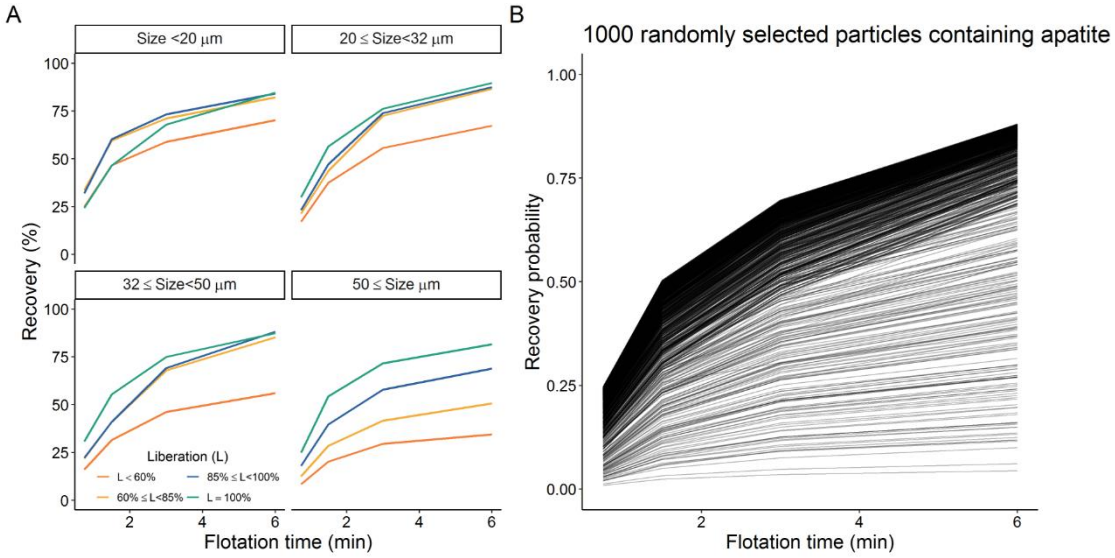

Figure 8: Recovery of particles containing apatite illustrated by the traditional particle binning method (A, Hoang et al., 2018) *and the novel particle based approach (B).*

The classical kinetic flotation model successfully described the particle recovery probability trend in the experiment demonstrated in this manuscript. It was selected following the discussion of Polat and Chander (2000) that advocate for the use of a simple flotation model and detailed particle classification. Future works can use the particle tracking approach of this manuscript to compute cumulative recovery probabilities for single particles, followed by testing different flotation kinetic models.

The lasso-regularization applied to the multinomial logistic regression permits identifying which particle properties are relevant in the mineral separation process (Hastie et al., 2015). We are thus able to input every particle property provided by the characterization system into the particle tracking model. The variable selection instrinsic to this method ultimately allows for a detailed analysis of how particle properties influence their flotation behavior.

In this manuscript, we used the modified flotation rate constant (k_m, Xu, 1998) to assess a particle's flotation performance. First, we were able to capture the well-described quasi-parabolic influence of size on the recoverability of apatite, dolomite, and calcite particles

(Figure 6) by true flotation (Wills and Finch, 2015), in agreement with the findings of Hoang et al. (2018). Following, we were able to jointly present the influence of shape, liberation and association on the recovery of apatite particles (Figure 7) and clearly recognize that non-liberated apatite particles have different flotation behavior according to their associated mineral. These findings expand the outcomes of many flotation studies that focused solely on the influence of surface liberation to explain a particle's recovery (Gorain et al., 2000; Hoang et al., 2018; Jameson, 2012; Lamberg and Vianna, 2007; Lotter et al., 2011). Moreover, we can highlight the importance of a holistic process understanding, in which no particle-descriptive variable is discarded before its relevance is systematically attested.

The recoverability of apatite particles with at least 70% free surface is very similar to that of the fully liberated particles, regardless of the associated minerals (Figures 6 and 7). Even though it translates into higher apatite recovery, it also poses a natural limitation to the highest obtainable grade, which could only be improved with regrinding.

Still in Figure 7, a bimodal distribution is observed for the intermediate apatite liberation bin (40% ≤ Liberation < 70%) irrespective of its association bin. Recalling the particle data treatment presented in Section 2.1, we add an interaction between shape and size descriptive variables and a categorical variable indicating the main mineral in mass of each particle. This strategy allows us to capture a mineral-specific effect of particle dimension properties on its recoverability. In this case, the particle dimension properties influence differently the process behavior of particles that have been grouped in the same liberation and association bins, but have different main mineral in mass. On the one hand, it leads to the bimodal distribution observed. On the other hand, it reinforces that the model is able to capture a unique influence of size for each mineral, similarly to what is observed for fully-liberated particles in Figure 6. Future studies should evaluate other strategies for the analysis of covariance model taking in consideration the limitations of the (multinomial) logistic regression.

The particle shape is recognized as one of the critical parameters in flotation. It influences the particle-bubble interactions in different levels: changes in surface area that lead to changes in surfactant coverage and finally to different levels of hydrophobicity; differences in flow velocity that leads to different attachment and detachment efficiencies. Most of the researchers advocate that non-spherical particles can float easier than the rounder particles (Verrelli et al., 2014). However, the findings of Little et al. (2016) and the studies of Schmidt and Berg (1997, 1996) showed an opposite behavior. Schmidt and Berg (1996) found that spherical printer toner particles floated better than disc or platy particles. They pointed out that, even though spheres are generally deflected away from bubbles by the flow stream (lower collision efficiency), they usually have a higher attachment efficiency. On the other hand, disc particles often collide with bubbles, but will end up bouncing off from it if the collision happens on the edge of the particle – leading to a lower overall flotation efficiency.

Particles of higher aspect ratio, hence the least elongated ones (Pourghahramani and Forssberg, 2005), have a higher chance of being recovered in the concentrate fraction irrespective of their constituting mineral, size and liberation (Figure 6). These findings are in agreement with the aforementioned studies (Little et al., 2016; Schmidt and Berg, 1997, 1996). This influence might be connected to the stability of coalescence, a combined effect of the particle-bubble collision hydrodynamics, the froth lamella drainage behavior, and the drop-back of previously attached particles from the froth. More test work is required for investigating these hypotheses.

We could not observe a significant effect of solidity in a particle's flotation behavior. It could mean either that a particle's solidity does not influence its recovery, or that the mineral liberation analyzer could not capture the particles' surface in sufficient detail in our case study. We recommend the future use of 3D mineral characterization systems (e.g. X-ray computed tomography, Ketcham and Carlson, 2001) for better investigating the influence of shape properties in the recovery of particles by flotation. Similarly to Pereira et al. (2020), our approach can promptly work with particle descriptive datasets from different characterization systems.

In the case study presented, flotation time was the only process variable involved. Further studies should explore the method's potential for comparing process outcomes under different machine setups. This approach can be used to identify optimum operating conditions and to understand the influence of machine/process parameters on particle recovery. As demonstrated by Pereira et al. (2020), this possibility is not limited to flotation but is extendable to any ore separation process.

Altogether, we anticipate that our method will assist further developments on the field of flotation given the resolution at which it allows the process to be observed. Moreover, the method is self-adaptive and has a good forecasting potential that can help the raw-materials sector thrive in a more sustainable use of raw materials through more efficient operations. The same is true for other methods borrowed from massive statistical and machine learning data analysis, such as the one presented here.

5 Acknowledgments

The authors thank the German Federal Ministry for Education and Research (BMBF) within the CLIENT-II initiative for funding this study (Grant number 033R189B). We thank our colleagues Markus Buchmann, Edgar Schach, Marius Kern, and Nathalie Kupka for fruitful discussions during method development.

Credit author contributions

Lucas Pereira: Conceptualization, Methodology, Software, Visualization. **Max Frenzel**: Conceptualization, Methodology, Supervision. **Duong Huu Hoang**: Investigation. **Raimon Tolosana-Delgado**: Methodology, Software. **Martin Rudolph**: Investigation. **Jens Gutzmer**: Supervision.

References

Bish, D.L., Post, J.E., 1989. Modern Powder Diffraction, Volume 20. ed, Reviews in Mineralogy volume 20. Mineralogical society of America, Chantilly, VA.

Dobby, G.S., Savassi, O.N., 2005. An advanced modelling technique for scale-up of batch flotation results to plant metallurgical performance. Australas. Inst. Min. Metall. Publ. Ser. 99–103.

Dowling, E.C., Klimpel, R.R., Aplan, F.F., 1985. Model Discrimination in the Flotation of a Porphyry Copper Ore. Trans. Am. Inst. Mining, Metall. Pet. Eng. Soc. 278, 87–102. https://doi.org/10.1007/bf03402602

Fandrich, R., Gu, Y., Burrows, D., Moeller, K., 2007. Modern SEM-based mineral liberation analysis. Int. J. Miner. Process. 84, 310–320. https://doi.org/10.1016/j.minpro.2006.07.018

Frenzel, M., Bachmann, K., Carvalho, J.R.S., Relvas, J.M.R.S., Pacheco, N., Gutzmer, J., 2019. The geometallurgical assessment of by-products—geochemical proxies for the complex mineralogical deportment of indium at Neves-Corvo, Portugal. Miner. Depos. 54, 959–982. https://doi.org/10.1007/s00126-018-0849-6

Friedman, J., Hastie, T., Tibshirani, R., 2010. Regularization Paths for Generalized Linear Models via Coordinate Descent. J. Stat. Software, Artic. 33, 1–22. https://doi.org/10.18637/jss.v033.i01

Gharai, M., Venugopal, R., 2015. Modeling of flotation process – an overview of different approaches. Miner. Process. Extr. Metall. Rev. 37, 08827508.2015.1115991. https://doi.org/10.1080/08827508.2015.1115991

Gorain, B.K., Franzidis, J.P., Ward, K., Johnson, N.W., Manlapig, E. V., 2000. Modeling of the Mount Isa rougherscavenger copper flotation circuit using size-by-liberation data. Miner. Metall. Process. 17, 173–180. https://doi.org/10.1007/bf03402844

Gu, Y., Schouwstra, R.P., Rule, C., 2014. The value of automated mineralogy. Miner. Eng. 58, 100–103. https://doi.org/10.1016/j.mineng.2014.01.020

Guilbert, J.M., Park, C.F., 2007. The Geology of Ore Deposits. Waveland Press.

Hastie, T., Tibshirani, R., Wainwright, M., 2015. Statistical Learning with Sparsity, Statistical Learning with Sparsity: The Lasso and Generalizations. Chapman and Hall/CRC. https://doi.org/10.1201/b18401

Heinig, T., Bachmann, K., Tolosana-Delgado, R., Boogaart, G. Van Den, Gutzmer, J., 2015. Monitoring gravitational and particle shape settling effects on MLA sampling preparation, in: IAMG Conference 2015. pp. 200–206.

Henderson, A.R., 2005. The bootstrap: A technique for data-driven statistics. Using computer-intensive analyses to explore experimental data. Clin. Chim. Acta 359, 1–26. https://doi.org/10.1016/j.cccn.2005.04.002

Hoang, D.H., Kupka, N., Peuker, U.A., Rudolph, M., 2018. Flotation study of fine grained carbonaceous sedimentary apatite ore – Challenges in process mineralogy and impact of hydrodynamics. Miner. Eng. 121, 196–204. https://doi.org/10.1016/j.mineng.2018.03.021

Jameson, G.J., 2012. The effect of surface liberation and particle size on flotation rate constants. Miner. Eng. 36-38, 132–137. https://doi.org/10.1016/j.mineng.2012.03.011

Jenkins, R., 2008. X-Ray Fluorescence Spectrometry, Handbook of Analytical Techniques. https://doi.org/10.1002/9783527618323.ch23

Keppel, G., Wickens, T.D., 2004. Design and Analysis: A Researcher's Handbook. Prentice Hall.

Kern, M., Möckel, R., Krause, J., Teichmann, J., Gutzmer, J., 2018. Calculating the deportment of a fine-grained and compositionally complex Sn skarn with a modified approach for automated mineralogy. Miner. Eng. 116, 213–225. https://doi.org/10.1016/j.mineng.2017.06.006

Ketcham, R. a., Carlson, W.D., 2001. Acquisition, optimization and interpretation of X-ray computed tomographic imagery: applications to the geosciences. Comput. Geosci. 27, 381–400. https://doi.org/10.1016/S0098-3004(00)00116-3

King, R.P., Schneider, C.L., King, E.A., 2012. Modeling and Simulation of Mineral Processing Systems, Second. ed. Society for Mining, Metallurgy, and Exploration, Englewood, California.

Kupka, N., Tolosana-Delgado, R., Schach, E., Bachmann, K., Heinig, T., Rudolph, M., 2020. R as an environment for data mining of process mineralogy data: A case study of an industrial rougher flotation bank. Miner. Eng. 146. https://doi.org/10.1016/j.mineng.2019.106111

Lamberg, P., Vianna, S., 2007. A technique for tracking multiphase mineral particles in flotation circuits. XXII Encontro Nac. Trat. Minérios e Metal. Extrativa - VII Meet. South. Hemisph. Miner. Technol. 195–202.

Leißner, T., Hoang, D.H.H., Rudolph, M., Heinig, T., Bachmann, K., Gutzmer, J., Schubert, H., Peuker, U.A. a., 2016. A mineral liberation study of grain boundary fracture based on measurements of the surface exposure after milling. Int. J. Miner. Process. 156, 3–13. https://doi.org/10.1016/j.minpro.2016.08.014

Little, L., Wiese, J., Becker, M., Mainza, A., Ross, V., 2016. Investigating the effects of particle shape on chromite entrainment at a platinum concentrator. Miner. Eng. 96-97, 46–52. https://doi.org/10.1016/j.mineng.2016.06.003

Lotter, N.O., Kormos, L.J., Oliveira, J., Fragomeni, D., Whiteman, E., 2011. Modern process mineralogy: Two case studies. Miner. Eng. 24, 638–650. https://doi.org/10.1016/j.mineng.2011.02.017

Pawlowsky-Glahn, V., Egozcue, J.J., Tolosana-Delgado, R., 2015. Modeling and Analysis of Compositional Data, Statistics in Practice. Wiley.

Pereira, L., Frenzel, M., Khodadadzadeh, M., Tolosana-Delgado, R., Gutzmer, J., 2020. A self-adaptive particle-tracking method for minerals processing. J. Clean. Prod. Under revi.

Petrucci, R.H., Herring, F.G., Bissonnette, C., Madura, J.D., 2016. General Chemistry: Principles and Modern Applications, 11th ed. Pearson Canada Incorporated.

Polat, M., Chander, S., 2000. First-order flotation kinetics models and methods for estimation of the true distribution of flotation rate constants. Int. J. Miner. Process. 58, 145–166. https://doi.org/10.1016/S0301-7516(99)00069-1

Pourghahramani, P., Forssberg, E., 2005. Review of applied particle shape descriptors and produced particle shapes in grinding environments. Part I: particle shape descriptors. Miner. Process. Extr. Metall. Rev. 26, 145–166. https://doi.org/10.1080/08827500590912095

R Core Team, 2017. R: A Language and Environment for Statistical Computing.

Runge, K., 2010. Laboratory flotation testing--an essential tool for ore characterisation, in: Flotation Plant Optimisation: A Metallurgical Guide to Identifying and Solving

Problems in Flotation Plants. Australasian Institute of Mining and Metallurgy, Spectrum Series Carlton, Vic, pp. 55–173.

Saerens, M., Latinne, P., Decaestecker, C., 2002. Adjusting the Outputs of a Classifier to New a Priori Probabilities: A Simple Procedure. Neural Comput. 14, 21–41. https://doi.org/10.1162/089976602753284446

Sandmann, D., 2015. Method Development in Automated Mineralogy. TU Bergakademie Freiberg.

Schmidt, D.C., Berg, J.C., 1997. A Preliminary Hydrodynamic Analysis of the Flotation of Disk-Shaped Toner Particles. Prog. Pap. Recycl. 6, 38–49.

Schmidt, D.C., Berg, J.C., 1996. The effect of particle shape on the flotation of toner particles. Prog. Pap. Recycl. 5, 67–77.

Sutherland, K.L., 1948. Physical chemistry of flotation. XI: Kinetics of the flotation process. J. Phys. Colloid Chem. 52, 394–425. https://doi.org/10.1021/j150458a013

Wills, B.A., Finch, J., 2015. Wills' Mineral Processing Technology: An Introduction to the Practical Aspects of Ore Treatment and Mineral Recovery. Elsevier Science.

Xu, M., 1998. Modified flotation rate constant and selectivity index. Miner. Eng. 11, 271–278. https://doi.org/10.1016/S0892-6875(98)00005-3

Annex 1

If the feed sample is also split into different size fractions, such as in the hypothetical experiment, its reconstruction can be done similarly to the products' procedure. The sole difference is that the statistical weight assigned to each feed's particle must sum up to the total number of particles in every size fraction of that sample. This requirement arises from the prior correction step (Saerens et al., 2002) of the particle tracking method, which is scale variant (Pereira et al., 2020). The statistical weight for the feed sample can be obtained by multiplying $SW_{p.sj}$ by the total number of particles present in every feed's size fraction datasets.

Table A 1: Hypothetical flotation experiment data. It contains the weight distribution, number of characterized particles, labels assigned for training each particle tracking model (PTM), and statistical weight of each particle ($SW_{p.sj}$) in each size fraction of the concentrates, tailings, and feed samples. Label "C" represents concentrate, "T" tailings, and "-" not used

Sample	Fraction (μm)	Wt. (%)	Particles nº	Label in each PTM		$SW_{p.sj}$	
				PTM 1	PTM 2	PTM1	PTM2
Concentrate 1	+ 50	10	150000	C	-	1.33E-06	-
	- 50	15	170000	C	-	1.76E-06	-
Concentrate 2	+ 50	15	155000	T	C	6.45E-07	1.94E-06
	- 50	10	165000	T	C	4.04E-07	1.21E-06
Tailings	+ 50	40	152000	T	T	1.75E-06	2.63E-06
	- 50	10	167000	T	T	3.99E-07	5.99E-07
Feed	+ 50	65	148000	-		1.38*	

	- 50	35	166000	-	0.66*

*The $SW_{p.sj}$ of the feed particles is normalized to the total number of particles in both size fraction samples

Table A 2: Weight distribution and number of particles characterized with the MLA in each flotation product. Additionally, the use of each fraction for training the four process models is displayed via the labels of each of them ("C" represents concentrate, "T" tailings, and "-" not used)

Fraction	Wt. (%)	Particle nº	Label in each PTM			
			PTM 1	PTM 2	PTM 3	PTM 4
CA -20	6.7	185952	C	-	-	-
CA +20-32	5.8	212465	C	-	-	-
CA +32-50	4.6	137023	C	-	-	-
CA +50	2.2	78712	C	-	-	-
CB -20	6.4	173513	T	C	-	-
CB +20-32	5.4	198645	T	C	-	-
CB +32-50	3.9	142061	T	C	-	-
CB +50	2.8	86449	T	C	-	-
CC -20	5.8	164071	T	T	C	-
CC +20-32	4.3	184961	T	T	C	-
CC +32-50	3.5	139719	T	T	C	-
CC +50	2.0	76500	T	T	C	-
CD -20	4.7	148161	T	T	T	C
CD +20-32	2.8	164470	T	T	T	C
CD +32-50	2.3	117546	T	T	T	C
CD +50	1.1	61203	T	T	T	C
TD -20	11.3	124433	T	T	T	T
TD +20-32	7.0	199521	T	T	T	T
TD +32-50	6.7	156597	T	T	T	T
TD +50	10.7	73710	T	T	T	T